frontiers | Frontiers in Catalysis

TYPE Original Research
PUBLISHED 17 May 2024
DOI 10.3389/fctls.2024.1353746

OPEN ACCESS

EDITED BY
Subhasis Shit,
Freie Universität Berlin, Germany

REVIEWED BY
Manisha Das,
CIC Energigune, Spain
Ivonne L. Alonso-Lemus,
Cinvestav Saltillo, Mexico

*CORRESPONDENCE
Jonathan Z. Bloh,
bloh@dechema.de

RECEIVED 09 February 2024
ACCEPTED 10 April 2024
PUBLISHED 17 May 2024

CITATION
Schanz T, Stöckl M, Burek BO, Holtmann D and Bloh JZ (2024), Combined anodic and cathodic peroxide production in an undivided carbonate/bicarbonate electrolyte with 144% combined current efficiency.
Front. Catal. 4:1353746.
doi: 10.3389/fctls.2024.1353746

Combined anodic and cathodic peroxide production in an undivided carbonate/bicarbonate electrolyte with 144% combined current efficiency

Tobias Schanz[1], Markus Stöckl[1], Bastien O. Burek[1], Dirk Holtmann[2] and Jonathan Z. Bloh[1]*

[1]DECHEMA-Forschungsinstitut, Frankfurt am Main, Germany, [2]Karlsruher Institut für Technologie, Institut für Bio- und Lebensmitteltechnik, Karlsruhe, Germany

In recent years, the electrochemical synthesis of peroxides has attracted renewed interest as a potential environmentally friendly production compared to the established anthraquinone process. In addition, it is possible to produce the peroxides directly on site, eliminating the need for expensive and hazardous transportation and storage. Cathodic production of hydrogen peroxide from oxygen is already quite well developed. Anodic production from water, on the other hand, is still facing significant challenges, despite its historic pioneering role. In this manuscript we show that anodic and cathodic synthesis of peroxides can even be combined to achieve greater than 100% current efficiency (CE) due to the combined effect of both half-reactions. So far, similar devices have always employed different electrolytes for each, which necessitated the use of a membrane and posed contamination risk. However, herein we show that both half-reactions can also employ the same electrolyte. This enables even an undivided cell, omitting the need for the expensive membranes. Despite its simplicity, this setup yielded an outstanding performance with a combined CE of 144%.

KEYWORDS

electrochemical peroxide production, paired electrolysis, percarbonates, hydrogen peroxide, membraneless cell

Introduction

Peroxides are important chemical compounds in many industries (Goor et al., 2012). The most widespread use is as a bleaching agent, for example, in the textile and paper industry (Goor et al., 2012). Peroxides are also employed as disinfectants in healthcare, as etching agent in the electronics industry or as oxidant for environmental remediation (Goor et al., 2012). In the chemical industry it is seen as the key compound for green oxidation chemistry (Sato, 2004; Russo et al., 2013; Ciriminna et al., 2016). The commercial production of hydrogen peroxide is almost exclusively done via the energy intensive anthraquinone process (17.6 kWh kg^{-1}_{H2O2}) (Goor et al., 2012; Sun et al., 2020; Pangotra et al., 2022a). Also, to make the process efficient, large, centralized plants are necessary which in turn means that the produced peroxide needs to be shipped over large distances to the typically decentral application sites.

However, over the past years, another option for the production of hydrogen peroxide has re-emerged. Once the pioneering technology for industrial hydrogen peroxide production, the electrochemical production from water and/or oxygen offers a promising alternative to the anthraquinone process (Wenderich et al., 2020). Particularly in terms of sustainability, as by using renewable power sources, the process does not emit any greenhouse gases. It is also possible to run small modular electrochemical peroxide systems in a decentralized matter, directly at the site of use. This further saves costs, resources and hazards associated with transportation and storage.

The electrochemical synthesis of hydrogen peroxide can take place by means of oxidation and/or reduction. At the cathode, molecular oxygen can be converted to hydrogen peroxide via a two-electron reduction reaction (2e-ORR), Eq. 1 (Siahrostami et al., 2020).

$$O_2 + 2\,H^+ + 2\,e^- \rightarrow H_2O_2 \quad E^0 = 0.68\,V \tag{1}$$

Several catalyst materials are currently known for the cathodic production of peroxide. Many of these materials are carbon-based and doped with other elements (Siahrostami et al., 2020). The majority of studies on the two-electron reduction reaction (2e-ORR) to hydrogen peroxide take place in an acidic environment due to the superior stability of H_2O_2 under these conditions. These include Pt/S doped carbon (Choi et al., 2016), $Au_{0.92}Pd_{0.08}$/carbon black (Jirkovský et al., 2011) and WO_3/vulcan carbon (Assumpção et al., 2013). Other works show that mesoporous carbon doped with nitrogen is able to produce H_2O_2 at a current efficiency (CE) of 95% in sulfuric acid solution (Sun et al., 2018) or the lowering of the overpotential by the modification of the electrode with carbon nanotubes (Bormann et al., 2019). Where given, the maximum concentration reported in these works ranged from 16 to 160 mM, where the latter appears to present an equilibrium concentration (Choi et al., 2016).

Some studies also employ alkaline electrolytes where carbon nanotubes (Gong et al., 2009) and mesoporous carbon (Kornienko et al., 2018) can achieve a current efficiency of 90%. Another reduction reaction in basic electrolyte is performed with doped carbon black (Sn_6Ni/carbon black) (Antonin et al., 2013). Carbon macrocycles with Co(II) phthalocyanine (Barros et al., 2013) und Fe(II) phthalocyanine (Silva et al., 2014) in potassium sulfate to achieve hydrogen peroxide FE of 80%. In general, carbon-based electrodes seem to perform reasonably well under near-neutral conditions (Holtmann et al., 2014). Another important type of cathode for reductive hydrogen peroxide production involves the deposition of anthraquinone on a carbon-based electrode. This work was performed in a 1 M $NaHCO_3$ solution (Jeon et al., 2020). This is particularly interesting as carbonate-containing electrolytes are very well suited for the anodic production of hydrogen peroxide (Fuku et al., 2016). In general, the fabrication and application of gas diffusion electrodes (GDE) represents the most desired type of electrodes for the cathodic half reaction. GDE allow high space-time-yields and allow to overcome solubility and transport limitations of oxygen in the electrolyte solution (Stöckl et al., 2023).

For anodic peroxide production, the challenge lies in controlling the reaction pathway. Only the 2-electron oxidation (2e-WOR, Eq. 2) to hydrogen peroxide is desirable, while both the overoxidation of the formed peroxide (Eq. 3) as well as the direct four-electron water oxidation to molecular oxygen (4e-WOR, Eq. 4) must be suppressed.

$$2\,H_2O \rightarrow H_2O_2 + 2\,H^+ + 2\,e^- \; E^0 = 1.76\,V \tag{2}$$

$$H_2O_2 \rightarrow O_2 + 2\,H^+ + 2\,e^- \; E^0 = 0.68\,V \tag{3}$$

$$2\,H_2O \rightarrow O_2 + 4\,H^+ + 4\,e^- \; E^0 = 1.23\,V \tag{4}$$

Typically, semiconducting metal oxides such as TiO_2, SnO_2, WO_3, and $BiVO_4$ are employed for this purpose due to their high oxygen but low hydroxyl binding energies (Siahrostami et al., 2017). In particular, many recent studies employed $BiVO_4$ using bicarbonate or carbonate electrolytes, both purely electrochemically but also photoelectrochemically (Shi et al., 2017; Xue et al., 2021). Based on this, bismuth vanadate was subsequently doped with different metals (Assumpção et al., 2013), (Baek et al., 2019) or coated with additional catalytic (Fuku and Sayama, 2016) and protective (Fuku et al., 2017a) metal oxide layers. In addition to the metal oxides already mentioned, other metal oxides such as MnOx (Izgorodin et al., 2012), $CaSnO_3$ (Park et al., 2019) or $InSbO_x$/$CuSb_2O_x$/FTO (Miyase et al., 2020) have been reported for anodic hydrogen peroxide synthesis. Beside metal oxides, small molecules like porphyrins (Kuttassery et al., 2017) or carbon based electrodes such as BDDs (Wenderich et al., 2021) or CFP (Pangotra et al., 2022b) have been used for the oxidation of water to hydrogen peroxide.

In addition to the catalyst materials, the choice of electrolyte also plays a decisive role. For example, Fuku et al. investigated the anodic hydrogen peroxide synthesis in different electrolytes and showed that the CE in potassium bicarbonate was significantly higher than in other electrolytes, presumably due to the catalytic role of the bicarbonate ion (Fuku and Sayama, 2016; Gill et al., 2021a). Gill et al. (2021b) later studied different composition of the carbonate buffer in more detail. A carbonate buffer with a $KHCO_3$ to K_2CO_3 ratio of 0.125 : 0.875 showed the highest performance, which made it possible to observe high efficiencies of about 50% CE even with longer measurements (up to 3 h). A possible reason for the high yields in carbonate-containing electrolytes is the oxidation of the electrolyte itself. For example, bicarbonate could be oxidized to peroxomonocarbonate (Siahrostami et al., 2017) and carbonate to peroxodicarbonate (Chardon et al., 2017). These could subsequently react with water to form hydrogen peroxide (Richardson et al., 2000; Bakhmutova-Albert et al., 2010). In general, one should assume that when using carbonate-containing solutions in connection with hydrogen peroxide, not only H_2O_2 is present, but a mixture of peroxo species (Zhao et al., 2018).

While both oxidative and reductive peroxide generation have mostly been combined with another balancing half-reaction, the obvious approach is to combine both in order to achieve a combined anodic-cathodic peroxide generation process. Such a process has the advantage that it does not produce potentially unwanted products at the other electrode and can achieve up to a combined theoretical current efficiency of 200%. Several approaches to realize this have been published in recent years. In an attempt to produce sodium percarbonate in both half-reactions, Ruiz et al. (2009) combined a BDD anode and carbon felt cathode in 1 M Na_2CO_3 electrolyte, separated by a cation-exchange membrane. However, they applied very high cell voltages of up to 10 V and only observed approximately 60% total peroxide formation efficiency, less than

what is typically observed with solely a GDE cathode. Another study also deals with the use of a peroxide-forming photoanode in combination with cathodic peroxide formation. Jeon et al. (2020) combined a P-Mo-co-doped $BiVO_4$ photoanode with an anthraquinone- and CNT-modified carbon cathode. They employed 1 M $NaHCO_3$ electrolytes for both half-reaction but separated by a Nafion membrane. However, due to the limited current at the photoanode (approx. 180 μA cm^{-2}), the maximum peroxide formation rate was very limited at 0.21 μmol cm^{-2} min^{-1} (Jeon et al., 2020). A similar attempt but with mixed electrolytes in both half-reactions has been reported but again with relatively low production rates of 0.48 μmol cm^{-2} min^{-1}, albeit at high CE of around 140% (Shi et al., 2018). Using an external bias potential, the production rate was increased to 7.3 μmol cm^{-2} min^{-1} (Shi et al., 2018).

All these studies have in common that they employ separated half-cells, sometimes even with different electrolytes. However, using different electrolytes (particularly with different pH values) is challenging and puts high demands on the employed membrane. Crossover is eventually inevitable and will cause a loss of efficiency or require frequent electrolyte regeneration. This would not be an issue if both half-reactions used the same electrolyte. In this case, it may also be possible to omit the membrane altogether, saving greatly on costs and complexity of the system. There are only few reports so far on such a system, for example, employing a $WO_3/BiVO_4$ photoanode and gold cathode in a shared 2 M $KHCO_3$ electrolyte (Fuku et al., 2017b). Unfortunately, they report only very short experiments of only a few minutes duration and just 200 μM of hydrogen peroxide formed so it is difficult to evaluate its feasibility and long-term performance. A particularly interesting system was published by Xia et al., which used a hydrophobized carbon paper anode in combination with a GDE in a membrane-free flow-cell using sodium carbonate electrolyte (Xia et al., 2020). They achieved a high specific production rate of 24 μmol min^{-1} at a CE of 144% but only used a very small anode (0.42 cm^2) and a very high electrolyte flow rate, leading to only diluted product solutions (maximum of 4.8 mM) (Xia et al., 2020). Unfortunately, the anode material also proved unstable and had to be replaced regularly in long-term experiments (Xia et al., 2020). Nonetheless, this report shows significant potential for membrane-less approaches. Ling et al. (2023) also reported a total CE of 153% in a combined approach, employing similar carbon-based electrodes and a Nafion membrane. In a membrane-free set-up, they achieved a CE of 136%, albeit with similar stability problems as the system only lasted for 4 h of operation.

We therefore investigated the feasibility of achieving an efficient membrane-less combined anodic-cathodic peroxide generation system using the same electrolyte for both half-reactions and a more stable oxide-based anode material (Figure 1).

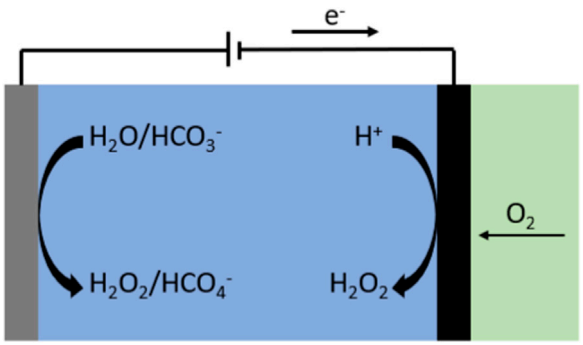

FIGURE 1
A schematic structure of the experimental cell with the respective reactions taking place. At the anode, water and hydrogen carbonate are oxidized to hydrogen peroxide and peroxymonocarbonate. At the cathode (GDE), hydrogen peroxide is reductively produced from oxygen gas supplied to the gas diffusion layer.

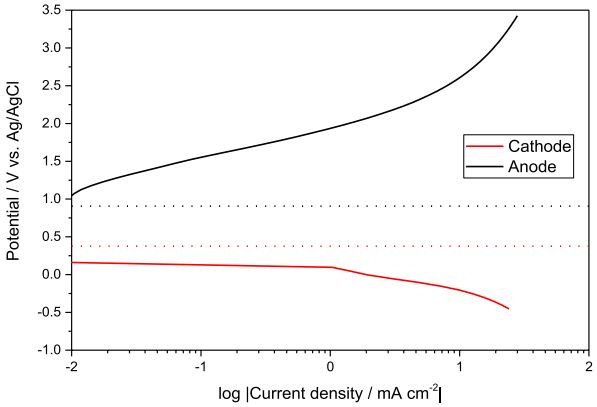

FIGURE 2
Electrode potential in dependence of the current density for both half-cells given in a half-logarithmic plot obtained via linear sweep voltammetry (LSV) in an unseparated cell with $InSbO_x/CuSb_2O_x$/FTO as anode (2.4 cm^{-2}) and a GDE with carbon black as cathode (geometrical area 4.9 cm^2). Polarization was performed against Ag/AgCl/KCl(sat.) in carbonate buffer under stirring with 0.5 M $KHCO_3$ and 3.5 M K_2CO_3 at a pH of 11.3. The cell volume was 120 mL of electrolyte solution. In the gas chamber of the GDE, humidified oxygen was offered in the GDE with an overpressure of 15 mbar. The dotted lines represent the equilibrium potentials for each reaction for these conditions (Siahrostami et al., 2020). See Supplementary Figures S5, S6 for the corresponding linear sweep voltammograms.

Results and discussion

To design an efficient peroxide generating cell that can operate using a shared electrolyte, the individual half-reactions were studied first. The electrolyte of choice is a concentrated carbonate electrolyte at pH 11.3 comprising 0.5 M $KHCO_3$ and 3.5 M K_2CO_3. This has so far been reported to achieve amongst the highest current efficiencies for anodic peroxide generation over BDD- and FTO-based anodes (Gill et al., 2021b). As anodes, $InSbO_x/CuSb_2O_x$ electrodes on FTO substrates (Supplementary Figure S1) were employed which have previously been reported as an efficient material at pH 8.3 in bicarbonate (Miyase et al., 2020). The often-reported $BiVO_4$ is not an option in this case as it is only stable up to about pH 10 (Kim and Lee, 2019).

As cathode, commercial gas diffusion electrodes (GDEs) from Gaskatel were used. The experiments were performed either in a single (membrane-less) or double (with membrane) H-cell (see Supplementary Figures S2–S4).

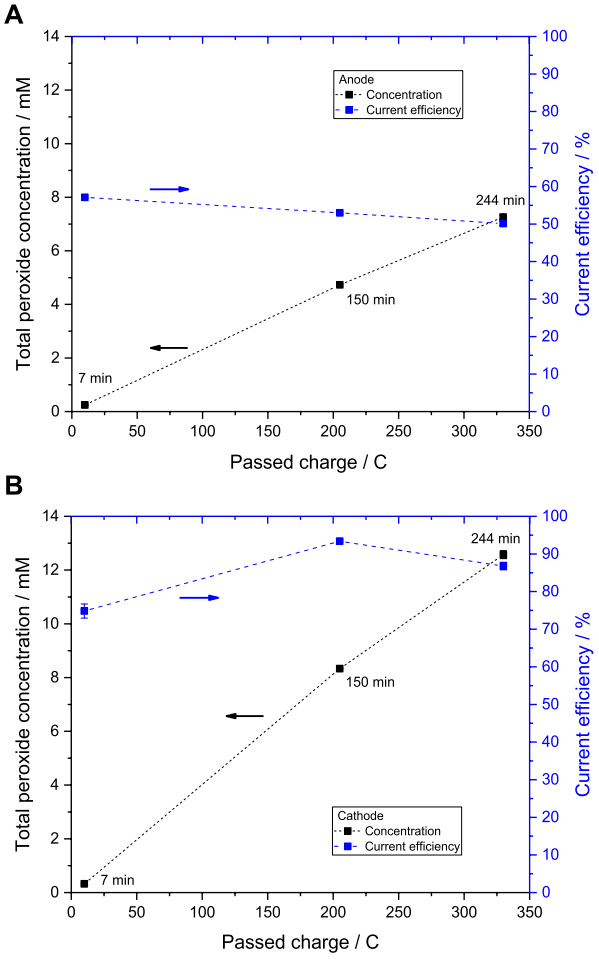

FIGURE 3
The total peroxide concentration and the CE plotted against the passed charge. **(A)** Peroxide production in the anode compartment of an $InSbO_x/CuSb_2O_x$/FTO electrode (2.4 cm^2). **(B)** Peroxide production in the cathode compartment of a GDE with carbon black (4.9 cm^{-2}). Chronocoulometry with $InSbO_x/CuSb_2O_x$/FTO as working electrode. Polarization was carried out at 2.385 V vs. Ag/AgCl (3.25 V vs. RHE) in stirred carbonate buffer with 0.5 M $KHCO_3$ and 3.5 M K_2CO_3 at a pH of 11.3. The anode and cathode compartments each contained 120 mL of electrolyte solution and were separated from one another by a cation exchange membrane. In the gas room of the GDE, humidified oxygen was offered at 15 mbar overpressure. The current during the experiment is shown in Supplementary Figure S7 for the anode. Error bars indicate the results of repeated peroxide analysis (n = 2–3) of this singular electrochemical experiment. For repeated experiments under these conditions, refer to Supplementary Figure S8. The interpolated lines between the data points only serve as a visual guide.

First, the current-voltage characteristics have been determined. As can be seen in Figure 2, the anode has a significantly higher overpotential than the cathode. At 0.1 mA cm^{-2} the anodic overpotential is 640 mV with a slope of 384 mV $decade^{-1}$ up to about 10 mA cm^{-2}, where it rapidly increases. In contrast, the cathode shows a modest overpotential of only 280 mV up to about 1 mA cm^{-2} with a shallower slope than the anode afterwards. Consequently, the anode was used as the working electrode in subsequent experiments due to its higher sensitivity to the applied voltage.

In the initial experiments, the strongly concentrated carbonate electrolyte led to precipitation or efflorescence of carbonate salts inside and on the gas-side surface of the GDE, quickly deactivating it. Presumably, this is a consequence of water evaporation into the oxygen gas stream and could be prevented by pre-humidifying the oxygen gas stream above the point of deliquescence for potassium carbonate (44% r.h.) (Kim et al., 1995). However, full water saturation (100% r.h.) is not recommended as it can lead to continuous water uptake of the electrolyte and "drowning" of the GDE. With the minor modification of gas pre-humidification, no major issues were encountered using the carbonate electrolyte for the cathode reaction.

Initial screening with $InSbO_x/CuSb_2O_x$ electrodes identified a potential of 2.385 V vs. Ag/AgCl as suitable for efficient anodic peroxide generation and was therefore used as a starting point for this study as well (Gill et al., 2021b). At this potential, a stable current density of about 10 mA cm^{-2} was achieved (Supplementary Figure S7). This is also the point where the overpotential starts to significantly increase (see Figure 2). Meanwhile, the potential of the cathode is at approx. −0.2 V vs. Ag/AgCl at this current density, estimated from the I-V curves. The total cell voltage is thus estimated at approx. 2.6 V.

Under these conditions, peroxides are generated both in the cathode and anode compartment in the divided cell using a cation exchange membrane (Figure 3). In both cases, the peroxide formation was linear over the investigated time of almost 4 h. Due to the electrolyte being concentrated carbonate, there will also be significant concentrations of percarbonates (peroxomonocarbonate, peroxodicarbonate) present alongside hydrogen peroxide. As the employed analytic methods are not specific for either, only total peroxide is discussed in the following. During the experiment (and also all subsequent ones), gas evolution was observable at the anode, presumably oxygen gas being formed from water (over)oxidation.

The cathode achieved almost quantitative peroxide formation with 86% CE at a final concentration of 12.5 mM (Figure 3B). Under the corresponding conditions, similar results could be achieved reproducibly with different amounts of charge.

The anode delivered a significantly lower current efficiency of 50%, yielding 7.3 mM peroxide during the experiment lasting until a charge of 330 C was passed. This lower performance is not surprising as the selective 2-electron water oxidation reaction is much more difficult to realize without significant overoxidation to oxygen. To prevent overoxidation, usually semiconducting electrodes are used which favor single electron transfer due to their much lower charge carrier density compared to metal or carbon-based electrodes (Beranek, 2019).

The carbonate electrolyte has also been reported to play a major role here. Presumably, carbonate and bicarbonate are adsorbed on the electrode surface and thereby reduce water coverage, suppressing the direct water oxidation. (Fan et al., 2022; Guo et al., 2022; Li et al., 2023). Instead, bicarbonate is directly oxidized to peroxomonocarbonate (HCO_4^-), either directly (Gill et al., 2021a) or via a carbonate radical (in carbonate-rich electrolytes such as the present one) (Fan et al., 2022), Eq. 5. The peroxomonocarbonate is subsequently partly hydrolyzed to form hydrogen peroxide, Eq. 6. However, due to the high concentration of both bicarbonate and carbonate in the electrolyte, there will always be significant

concentrations of peroxomonocarbonate as well as peroxodicarbonate ($C_2O_6^{2-}$) present in equilibrium alongside hydrogen peroxide (Schanz et al., 2023).

$$HCO_3^- + H_2O \rightarrow HCO_4^- + 2H^+ + 2e^- \quad (5)$$

$$HCO_4^- + H_2O \rightarrow HCO_3^- + H_2O_2 \quad (6)$$

As the electrodes are well-covered by carbonate (Gill et al., 2021b), direct (over-)oxidation of hydrogen peroxide is suppressed, resulting in the higher observed peroxide selectivity. Additionally, the formed percarbonates may also be more resistant to overoxidation than hydrogen peroxide itself.

Since the substrate of the anode (FTO) itself has also a demonstrated activity for anodic peroxide formation (Fan et al., 2022), a control experiment using bare FTO as the anode was performed. However, this electrode has a significantly later onset and therefore only yielded less than half of the current density (4.5 mA cm^{-2}) and a reduced CE of 39% (Supplementary Figure S9) under the same reaction conditions. This proves that indeed the $InSbO_x/CuSb_2O_x$ coating plays a critical role for the anode performance.

If both half-cells are taken together, the total combined current efficiency amounts to 138%. The average peroxide concentration was 9.9 mM but with a higher concentration in the cathode compartment. This already demonstrates that higher-than-unity efficiency is possible for electrochemical peroxide production. Interestingly, in these experiments no sign of deactivation or decreased activity at higher peroxide concentrations was yet observed.

Since presumably, both in the anode and the cathode, the same species are formed (hydrogen peroxide, peroxomonocarbonate, peroxodicarbonate), this begs the question if the membrane is actually needed to prevent electrolyte mixing. An undivided cell is particularly interesting for technical applications since the membrane does not only present a significant cost factor, (Krishnan et al., 2023), but also increases cell resistance, sealing points and may reduce cell lifetime. (Hadikhani et al., 2021). Therefore, membrane-less cell are significantly easier and less expensive to produce. Therefore, the next set of experiments was conducted in an undivided cell without a membrane. The polarization was carried out under the same conditions as those with a membrane (anode potential 2.385 V vs. Ag/AgCl, current density of about 10 mA cm^{-2}). This time, however, the anode and cathode reactions took place in a shared reaction chamber and were not separated from one another by a membrane.

As illustrated in Figure 4, this configuration achieved a combined CE of 144%, showing virtually the same combined efficiency as in the case of the divided cell. During the reaction, a concentration of 35.5 mM was reached, the higher concentration being due to a longer experimental period, but also a lower electrolyte volume compared to the divided cell. Over the course of the experiment (up to 560 C), the peroxide concentration increased linearly, with the CE being nearly constant. Again, no significant reduction in the current density was observed over the course of more than 6 h (Supplementary Figure S10), indicating that the system is stable, and the electrodes do not degrade under these conditions. These results correspond to a remarkable production rate of 4.41, 2.16 or 1.45 µmol cm^{-2} min^{-1} depending on whether only the active area of the anode, GDE or both combined are taken as reference.

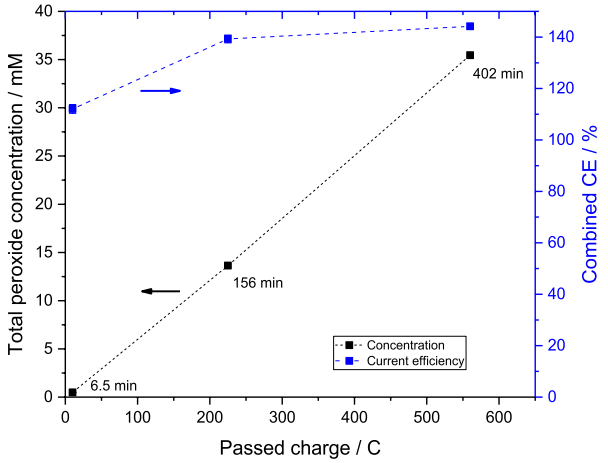

FIGURE 4
Total formed peroxide over passed charge, using an $InSbO_x/CuSb_2O_x$/FTO electrode (2.4 cm^2) as anode. A GDE with carbon black (4.9 cm^{-2}) was used as the cathode. Polarization was carried out at 2.385 V vs. Ag/AgCl (3.25 V vs. RHE) with the anode as working electrode in carbonate buffer while stirring with 0.5 M $KHCO_3$ and 3.5 M K_2CO_3 at a pH of 11.3. The undivided electrode compartment contained 120 mL of electrolyte solution. In the gas room of the GDE, humidified oxygen was offered at 15 mbar overpressure. The current during the experiment is shown in Supplementary Figure S10. Error bars indicate the results of repeated peroxide analysis (n = 2–3) of this singular electrochemical experiment. For repeated experiments under these conditions, refer to Supplementary Figure S11. The interpolated lines between the data points only serve as a visual guide.

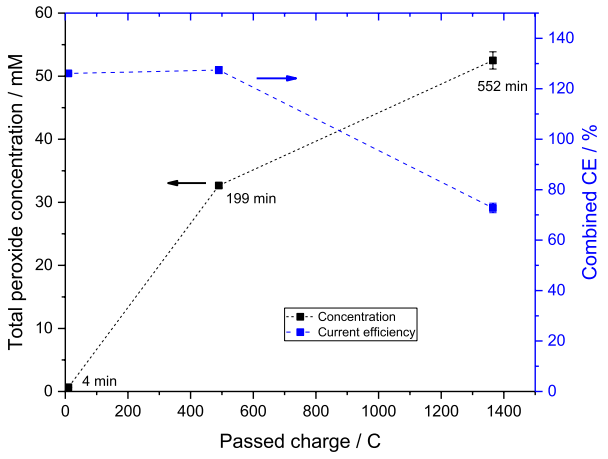

FIGURE 5
Total formed peroxide over passed charge, using an $InSbO_x/CuSb_2O_x$/FTO electrode (2.4 cm^2) as anode. A GDE with carbon black (4.9 cm^2) was used as the cathode. Polarization was carried out at 3 V vs. Ag/AgCl (3.85 V vs. RHE) in stirred carbonate buffer with 0.5 M $KHCO_3$ and 3.5 M K_2CO_3 at a pH of 11.3. The electrode compartment contained 100 mL of electrolyte solution. In the gas room of the GDE, humidified oxygen was offered at 15 mbar overpressure. The current during the experiment is shown in Supplementary Figure S12. Error bars indicate the results of repeated peroxide analysis (n = 2–3) of this singular electrochemical experiment. For repeated experiments under these conditions, refer to Supplementary Figure S13. The interpolated lines between the data points only serve as a visual guide.

Using the estimated cell voltage of 2.6 V (estimated from the half-cell U-I-curves, see Figure 2) as a basis, the overall energy efficiency for peroxide production is 29% in the present case, the specific energy demand being 10.05 MJ kg^{-1} or 2.79 kWh kg^{-1} (hydrogen peroxide equivalent). This is significantly less than the current production process (anthraquinone process) at 17.6 kWh kg^{-1} and thus presents a very favorable alternative (Pangotra et al., 2022a). Previous studies on the purely anodic peroxide electrolysis also reported significantly higher specific energy consumption of 13–40 kWh kg^{-1}, albeit at much higher current densities (Pangotra et al., 2022a).

Overall, this is about the same performance that was previously observed in the divided cell, suggesting that the membrane is indeed superfluous, and its omission does not have any immediately apparent detrimental effects. However, negative effects may arise at higher peroxide concentration and/or higher potentials which both favor peroxide decomposition.

Therefore, the anode was operated at a higher potential of 3 V vs. Ag/AgCl next (corresponding to a cell voltage of approx. 3.35 V based on the half-cell U-I-curves) in a subsequent experiment (Figure 5). This resulted in a much higher current density of 17 mA cm^{-2}, which again proved very stable over several hours (Supplementary Figure S12). The initially observed combined CE was slightly lower but still above unity at 125%, indicating that the higher potential leads to a slightly higher rate of overoxidation and thereby lower efficiency.

Due to the increased current density resulting from the higher potential applied at the anode, this experiment also yielded higher peroxide concentrations in the same timeframe, exceeding 50 mM. Up to a concentration of about 35 mM, the current efficiency stayed constant, but then began to level off with reduced efficiency so that the last data point with 52.5 mM only affords a combined CE of 72%. Kinetic analysis using a simple zero order formation, first order degradation approach (Burek et al., 2019) estimates the equilibrium concentration at around 58 mM, which is similar to what has been observed for BDD anodes (Pangotra et al., 2022a).

Due to the higher current density and only moderately lower efficiency, the production rate in this case reached even higher values of 2.24 µmol cm^{-2} min^{-1} calculated with the combined electrode surface area. However, this value was obtained after 490 C, in longer experiments the production rate drops alongside the efficiency. The energy efficiency is significantly lower in this case at 20%, both due to the reduced CE and the higher cell voltage. Even though the specific energy demand is still rather low in this case with 4.11 kWh kg^{-1}, this highlights that for higher current densities, more efficient catalysts and electrode designs are required to combat the steep increase in cell voltage seen here for >10 mA cm^{-2}, particularly at the anode.

Conclusion

The combination of anodic and cathodic peroxide production would be an ideal way to make the process more efficient, as a combined current efficiency of up to 200% can be achieved by replacing the other unproductive half-reaction (water oxidation to oxygen). However, so far this has only been realized with a fraction of the efficiency and in different electrolyte systems, which require a suitable and expensive membrane. We have shown that the cathodic peroxide generation is also possible with high efficiency using a gas-diffusion electrode in the carbonate/bicarbonate electrolyte solution, which is the current state-of-the-art electrolyte solution in anodic peroxide production. This reduces the requirements of the membrane as cross-over will no longer be a major concern. Interestingly, even completely omitting the membrane and working in a shared electrolyte did not show any significant detrimental effects. This greatly reduces the complexity and costs of the resulting devices and eliminates the membrane resistance.

Overall, the combination of the highly efficient cathodic process with a CE of up to 93% and the anodic peroxide process with up to 57% CE resulted in a combined efficiency of up to 144%, which represents a new benchmark for membrane-less combined peroxide synthesis using oxide-based anode materials. In the measurements shown here, both processes demonstrate that they are stable for at least several hours and show a linear peroxide formation rate. Further experiments showed reproducible results. In the measurements shown here, the efficiency only decreases at concentrations upwards of 35 mM, where overoxidation most likely begins to reduce the overall efficiency. The highest peroxide concentration achieved in the membrane-less cell in the measurements shown here was 52.5 mM, which equals 1.8 g L^{-1} or 0.18 wt.%. The specific energy demand for peroxide production was very low at only 2.8 kWh kg^{-1} in the best case, which is far below the value of the current anthraquinone production process (17.6 kWh kg^{-1}) (Pangotra et al., 2022a). This demonstrates the immense potential of electrochemical peroxide synthesis to improve efficiency and reduce costs for peroxides.

While the achieved concentrations seems still too low for many applications and likely requires further processing to achieve higher concentrations, it should be kept in mind that due to the carbonate electrolyte system, significant concentrations of percarbonates (peroxomonocarbonate, peroxodicarbonate) will be present (Ruiz et al., 2009; Schanz et al., 2023). These have much higher reaction rates than hydrogen peroxide versus many target compounds, e.g., 300-fold vs. sulfides (Richardson et al., 2000) or 250-fold vs. methylene blue (Schanz et al., 2023), so the reactivity (and thereby usability) of the as-prepared peroxide solutions from this process may be much higher than the concentration implies. Future optimization should focus on further increasing the anode current efficiency and suppressing the overoxidation of the peroxides to improve the overall process efficiency and enable higher maximum concentrations. Higher current densities are also desired for industrial applications, however, it has already been shown that industrially relevant current densities are achievable in similar systems (Fan et al., 2022).

Experimental details

Peroxide quantification method

As peroxide quantification method we used a colorimetric iodometry method (Xiao et al., 2019). For this purpose, 100 µL of a sample taken from the electrolyte were mixed with 135 µL pH 4.1 potassium phosphate (Carl Roth) buffer, 10 µL 1.2 M potassium iodide (Alfa Aesar) solution and 5 µL of a 35 mM Mo^{VI} solution [Ammonium molybdate (VI) tetrahydrate, Acros Organics] into a 96-well plate (F-Well, transparent, polystyrene).

The absorbance of the resulting triiodide can then be measured at 350 nm and compared to that of a calibration with an H_2O_2 standard (concentration range 5–70 µM) in this electrolyte solution (Supplementary Figure S14). As previously established, this method detects both hydrogen peroxide and percarbonates indiscriminately (Zhao et al., 2018).

Preparation of $InSbO_x/CuSb_2O_x$/FTO anodes

The $InSbO_x/CuSb_2O_x$/FTO electrodes were manufactured using spin coating followed by calcination (Jeon et al., 2020). First, the FTO substrates (Sigma-Aldrich, 2.3 mm thickness, surface resistivity 7 Ω/sq) were cleaned in an acetone/water mixture (50:50) using an ultrasonic bath. Then the $CuSb_2O_x$ precursor solution was first applied to the substrate by means of spin-coating (POLOS SPIN150i, 1,000 rpm, 15 s, 30 µL cm^{-2}). After applying the precursor solution, the substrates were calcined in air at 973 K for 30 min. After applying the $CuSb_2O_x$ layer, the $InSbO_x$ layer was applied with the same parameters. The subsequent calcination took place at 923 K for 30 min. The preparation of the $CuSb_2O_x$ precursor solution was accomplished by dispersing the respective metal oxides (CuO-200 mesh powder and Sb_2O_5 obtained from Thermo Fisher Scientific) at a concentration of 0.2 M total concentration in an Sb/Cu molar ratio of 2.0, in butyl acetate. The $InSbO_x$ precursor solution was prepared in the same way with In_2O_3 (obtained from Thermo Fisher Scientific, −325 mesh powder) and Sb_2O_5, but the ratio of the two metals to each other is 1:1. The corresponding electrode was contacted with an alligator clip (Supplementary Figure S15).

Preparation of gas diffusion electrodes

The cathode was a carbon black GDE from gaskatel (PerOx, Hydrogen peroxide electrode with PTFE layer). For the experiments, the PTFE layer on the GDE was carefully peeled off by hand as the high hydrophobicity was not needed in the small cell. A suitable piece of the electrode was then cut out and inserted into the H-cell.

Electrochemical experiments

The electrochemical experiments were carried out in a single or double H-cell glass reactor similar to those reported before Klein et al. (2023), Schneider and Stöckl (2024). Two or three 100 mL cylindrical capped flasks were customized with horizontal glass flanges which were used to connect them (see Supplementary Figures S2–S4) and secured with clamps. In the case of the separated cell, 3 flasks were used (see Supplementary Figures S2B, S3). The left flask (anode chamber) contained the anode ($InSbO_x/CuSb_2O_x$/FTO slides, 2.4 cm^2) which was directly immersed in the electrolyte comprising 0.5 M $KHCO_3$ and 3.5 M K_2CO_3 (pH = 11.3). The middle flask (cathode chamber) contained the same electrolyte, and the membrane (Fumatech fumasep F-10120-PK, 4.9 cm^2) was sandwiched between the flanges of the anode and cathode chambers. The cathode was a gas-diffusion electrode (gaskatel, 4.9 cm^2), which was sandwiched between the flanges of the cathode and gas chambers (right flask). The latter contained only oxygen, to humidify the oxygen gas stream prior to supplying it to the GDE cathode, it was passed through a water column. Similarly, 15 mbar of overpressure was realized with the pressure of a water column at the outlet of the gas stream. Both the anode and cathode chambers were stirred using a magnetic stirring bar. In the case of the membrane-less setup, only two flasks were employed (see Supplementary Figures S2A, S4). In this case, the membrane and the cathode chamber were omitted. Instead, the gas diffusion electrode (cathode) is located between the anode and gas chamber. The experiments were run with a Zahner Zennium-E4 potentiostat at a constant potential of 2.385 V or 3 V vs. Ag/AgCl (chronocoulometry). The electrochemical experiments were all performed at room temperature and with stirring. The reference electrode was an Ag/AgCl electrode with saturated KCl solution (Meinsberg, SE21-L), which was positioned with a luggin capillary directly in front of the respective working electrode (Supplementary Figure S2). The current curves and duration of the respective experiments can be found in the Supplementary Figures S7, S9, S10, S12. In the LSV measurements, starting from 0 V vs. Ag/AgCl, the potential was increased by 50 mV s^{-1} anodically (up to 3.5 V vs. Ag/AgCl) and cathodically (down to −0.5 V vs. Ag/AgCl).

Calculation of energy efficiency

Energy efficiency of peroxide formation (*EE*) was calculated as follows. For simplicity, we assume all products are hydrogen peroxide. The decomposition/combustion enthalpy ($\Delta_c H^0$) of H_2O_2 is −98 kJ mol^{-1} (calculated from heats of formation) (Haynes, 2010) and was taken as measure for the energy stored in the products, together with the amount of formed peroxide (n_{H2O2}). Energy input is calculated according to the cell voltage (U) and the passed charge (q):

$$EE = \frac{n_{H2O2} \cdot -\Delta_c H^0}{q \cdot U}$$

Specific energy consumption per product formed (E_{H2O2}) was calculated similarly using the molecular mass of hydrogen peroxide (m_{H2O2}):

$$E_{H2O2} = \frac{q \cdot U}{n_{H2O2} \cdot m_{H2O2}}$$

Data availability statement

The original contributions presented in the study are included in the article/Supplementary Material, further inquiries can be directed to the corresponding author.

Author contributions

TS: Conceptualization, Data curation, Investigation, Methodology, Visualization, Writing–original draft, Writing–review and editing. MS: Conceptualization, Methodology, Writing–review and editing. BB: Conceptualization, Supervision, Writing–review and editing. DH: Conceptualization, Methodology, Writing–review and editing. JB: Conceptualization, Funding acquisition, Methodology, Project administration, Supervision, Writing–original draft, Writing–review and editing.

Funding

The authors declare that financial support was received for the research, authorship, and/or publication of this article. The authors are grateful for financial support by the German Ministry of Education and Research (BMBF) within the project "CO_2SimO" (grant no. 033RC029C).

Conflict of interest

The authors declare that the research was conducted in the absence of any commercial or financial relationships that could be construed as a potential conflict of interest.

Publisher's note

All claims expressed in this article are solely those of the authors and do not necessarily represent those of their affiliated organizations, or those of the publisher, the editors and the reviewers. Any product that may be evaluated in this article, or claim that may be made by its manufacturer, is not guaranteed or endorsed by the publisher.

Supplementary material

The Supplementary Material for this article can be found online at: https://www.frontiersin.org/articles/10.3389/fctls.2024.1353746/full#supplementary-material

References

Antonin, V. S., Assumpcao, M. H. M. T., Silva, J. C. M., Parreira, L. S., Lanza, M. R. V., and Santos, M. C. (2013). Synthesis and characterization of nanostructured electrocatalystsbased on nickel and tin for hydrogen peroxide electrogeneration. *Electrochim. Acta* 109, 245–251. doi:10.1016/j.electacta.2013.07.078

Assumpção, M. H. M. T., De Souza, R. F. B., Reis, R. M., Rocha, R. S., Steter, J. R., Hammer, P., et al. (2013). Low tungsten content of nanostructured material supported on carbon for the degradation of phenol. *Appl. Catal. B Environ.* 142–143, 479–486. doi:10.1016/j.apcatb.2013.05.024

Baek, J. H., Gill, T. M., Abroshan, H., Park, S., Shi, X., Nørskov, J., et al. (2019). Selective and efficient Gd-doped BiVO 4 photoanode for two-electron water oxidation to H 2 O 2. *ACS Energy Lett.* 4 (3), 720–728. doi:10.1021/acsenergylett.9b00277

Bakhmutova-Albert, E. V., Yao, H., Denevan, D. E., and Richardson, D. E. (2010). Kinetics and mechanism of peroxymonocarbonate formation. *Inorg. Chem.* 49 (24), 11287–11296. doi:10.1021/ic1007389

Barros, W. R. P., Reis, R. M., Rocha, R. S., and Lanza, M. R. V. (2013). Electrogeneration of hydrogen peroxide in acidic medium using gas diffusion electrodes modified with cobalt (II) phthalocyanine. *Electrochim. Acta* 104, 12–18. doi:10.1016/j.electacta.2013.04.079

Beranek, R. (2019). Selectivity of chemical conversions: do light-driven photoelectrocatalytic processes hold special promise? *Angew. Chem.* 131 (47), 16878–16883. doi:10.1002/ange.201908654

Bormann, S., van Schie, M. M. C. H., De Almeida, T. P., Zhang, W., Stöckl, M., Ulber, R., et al. (2019). H2O2 production at low overpotentials for electroenzymatic halogenation reactions. *ChemSusChem* 12 (21), 4759–4763. doi:10.1002/cssc.201902326

Burek, B. O., Bahnemann, D. W., and Bloh, J. Z. (2019). Modeling and optimization of the photocatalytic reduction of molecular oxygen to hydrogen peroxide over titanium dioxide. *ACS Catal.* 9 (1), 25–37. doi:10.1021/acscatal.8b03638

Chardon, C. P., Matthée, T., Neuber, R., Fryda, M., and Comninellis, C. (2017). Efficient electrochemical production of peroxodicarbonate applying DIACHEM® diamond electrodes. *ChemistrySelect* 2 (3), 1037–1040. doi:10.1002/slct.201601583

Choi, C. H., Kim, M., Kwon, H. C., Cho, S. J., Yun, S., Kim, H.-T., et al. (2016). Tuning selectivity of electrochemical reactions by atomically dispersed platinum catalyst. *Nat. Commun.* 7 (1), 10922. doi:10.1038/ncomms10922

Ciriminna, R., Albanese, L., Meneguzzo, F., and Pagliaro, M. (2016). Hydrogen peroxide: a key chemical for today's sustainable development. *ChemSusChem* 9 (24), 3374–3381. doi:10.1002/cssc.201600895

Fan, L., Bai, X., Xia, C., Zhang, X., Zhao, X., Xia, Y., et al. (2022). CO2/Carbonate-Mediated electrochemical water oxidation to hydrogen peroxide. *Nat. Commun.* 13 (1), 2668. doi:10.1038/s41467-022-30251-5

Fuku, K., Miyase, Y., Miseki, Y., Funaki, T., Gunji, T., and Sayama, K. (2017b). Photoelectrochemical hydrogen peroxide production from water on a WO 3/BiVO 4 photoanode and from O 2 on an Au cathode without external bias. *Chem. - Asian J.* 12 (10), 1111–1119. doi:10.1002/asia.201700292

Fuku, K., Miyase, Y., Miseki, Y., Gunji, T., and Sayama, K. (2016). Enhanced oxidative hydrogen peroxide production on conducting glass anodes modified with metal oxides. *ChemistrySelect* 1 (18), 5721–5726. doi:10.1002/slct.201601469

Fuku, K., Miyase, Y., Miseki, Y., Gunji, T., and Sayama, K. (2017a). WO3/BiVO4 photoanode coated with mesoporous Al2O3 layer for oxidative production of hydrogen peroxide from water with high selectivity. *RSC Adv.* 7 (75), 47619–47623. doi:10.1039/c7ra09693c

Fuku, K., and Sayama, K. (2016). Efficient oxidative hydrogen peroxide production and accumulation in photoelectrochemical water splitting using a tungsten trioxide/bismuth vanadate photoanode. *Chem. Commun.* 52 (31), 5406–5409. doi:10.1039/c6cc01605g

Gill, T. M., Vallez, L., and Zheng, X. (2021a). The role of bicarbonate-based electrolytes in H2O2Production through two-electron water oxidation. *ACS Energy Lett.* 6 (8), 2854–2862. doi:10.1021/acsenergylett.1c01264

Gill, T. M., Vallez, L., and Zheng, X. (2021b). Enhancing electrochemical water oxidation toward H2O2via carbonaceous electrolyte engineering. *ACS Appl. Energy Mater.* 4 (11), 12429–12435. doi:10.1021/acsaem.1c02258

Gong, K., Du, F., Xia, Z., Durstock, M., and Dai, L. (2009). Nitrogen-doped carbon nanotube arrays with high electrocatalytic activity for oxygen reduction. *Science* 323 (5915), 760–764. doi:10.1126/science.1168049

Goor, G., Glenneberg, J., and Jacobi, S. (2012). "Ullmann's encyclopedia of industrial chemistry: hydrogen peroxide," in *Ullmann's encyclopedia of industrial chemistry* (Weinheim, Germany: Wiley-VCH Verlag GmbH and Co. KGaA), 393–427.

Guo, W., Xie, Y., Tang, S., Yu, B., Lian, X., Henkelman, G., et al. (2022). H2O2 formation mechanisms on the (1 1 2) and (3 1 0) facets of SnO2 via water oxidation reaction with the participation of bicarbonate: DFT and experimental investigations. *Appl. Surf. Sci.* 596, 153634. doi:10.1016/j.apsusc.2022.153634

Hadikhani, P., Hashemi, S. M. H., Schenk, S. A., and Psaltis, D. (2021). A membraneless electrolyzer with porous walls for high throughput and pure hydrogen production. *Sustain. Energy Fuels* 5 (9), 2419–2432. doi:10.1039/d1se00255d

Haynes, W. M. (2010) *Handbook of chemistry and physics*. 91th Edition. Boca Raton: CRC Press.

Holtmann, D., Krieg, T., Getrey, L., and Schrader, J. (2014). Electroenzymatic process to overcome enzyme instabilities. *Catal. Commun.* 51, 82–85. doi:10.1016/j.catcom.2014.03.033

Izgorodin, A., Izgorodina, E., and MacFarlane, D. R. (2012). Low overpotential water oxidation to hydrogen peroxide on a MnO x catalyst. *Energy Environ. Sci.* 5 (11), 9496–9501. doi:10.1039/c2ee21832a

Jeon, T. H., Kim, H., Kim, H. I., and Choi, W. (2020). Highly durable photoelectrochemical H2O2 production: via dual photoanode and cathode processes under solar simulating and external bias-free conditions. *Energy Environ. Sci.* 13 (6), 1730–1742. doi:10.1039/c9ee03154e

Jirkovský, J. S., Panas, I., Ahlberg, E., Halasa, M., Romani, S., and Schiffrin, D. J. (2011). Single atom hot-spots at Au-Pd nanoalloys for electrocatalytic H 2O 2 production. *J. Am. Chem. Soc.* 133 (48), 19432–19441. doi:10.1021/ja206477z

Kim, J. H., and Lee, J. S. (2019). Elaborately modified BiVO4 photoanodes for solar water splitting. *Adv. Mater.* 31 (20), 18069388–e1807035. doi:10.1002/adma.201806938

Kim, Y. P., Seinfeld, J. H., and Saxena, P. (1995). Atmospheric gas-aerosol equilibrium: IV. Thermodynamics of carbonates. *Aerosol Sci. Technol.* 23 (2), 131–154. doi:10.1080/02786829508965300

Klein, J., Kupec, R., Stöckl, M., and Waldvogel, S. R. (2023). Degradation of lignosulfonate to vanillic acid using ferrate. *Adv. Sustain. Syst.* 7 (4). doi:10.1002/adsu.202200431

Kornienko, V. L., Kolyagin, G. A., Kornienko, G. V., Parfenov, V. A., and Ponomarenko, I. V. (2018). Electrosynthesis of H2O2 from O2 in a gas-diffusion electrode based on mesostructured carbon CMK-3. *Russ. J. Electrochem.* 54 (3), 258–264. doi:10.1134/S1023193518030060

Krishnan, S., Koning, V., Theodorus de Groot, M., de Groot, A., Mendoza, P. G., Junginger, M., et al. (2023). Present and future cost of alkaline and PEM electrolyser

stacks. *Int. J. Hydrogen Energy* 48 (83), 32313–32330. doi:10.1016/j.ijhydene.2023.05.031

Kuttassery, F., Mathew, S., Sagawa, S., Remello, S. N., Thomas, A., Yamamoto, D., et al. (2017). One electron-initiated two-electron oxidation of water by aluminum porphyrins with earth's most abundant metal. *ChemSusChem* 10 (9), 1909–1915. doi:10.1002/cssc.201700322

Li, L., Hu, Z., Kang, Y., Cao, S., Xu, L., Yu, L., et al. (2023). Electrochemical generation of hydrogen peroxide from a zinc gallium oxide anode with dual active sites. *Nat. Commun.* 14 (1), 1890–1912. doi:10.1038/s41467-023-37007-9

Ling, C., Liang, A., Li, C., and Wang, W. (2023). Coupling functional anodes with natural air-diffused cathodes enables highly efficient hydrogen peroxide electrosynthesis. *J. Zhejiang Univ. Sci. A* 24 (4), 377–386. doi:10.1631/jzus.A2200566

Miyase, Y., Miseki, Y., Gunji, T., and Sayama, K. (2020). Efficient H2O2 production via H2O oxidation on an anode modified with Sb-containing mixed metal oxides. *Chem Electro Chem* 7 (11), 2448–2455. doi:10.1002/celc.202000276

Pangotra, D., Csepei, L. I., Roth, A., Ponce de León, C., Sieber, V., and Vieira, L. (2022b). Anodic production of hydrogen peroxide using commercial carbon materials. *Appl. Catal. B Environ.* 303, 120848. doi:10.1016/j.apcatb.2021.120848

Pangotra, D., Csepei, L.-I., Roth, A., Sieber, V., and Vieira, L. (2022a). Anodic generation of hydrogen peroxide in continuous flow. *Green Chem.* 24 (20), 7931–7940. doi:10.1039/d2gc02575b

Park, S. Y., Abroshan, H., Shi, X., Jung, H. S., Siahrostami, S., and Zheng, X. (2019). CaSnO 3: an electrocatalyst for two-electron water oxidation reaction to form H 2 O 2. *ACS Energy Lett.* 4 (1), 352–357. doi:10.1021/acsenergylett.8b02303

Richardson, D. E., Yao, H., Frank, K. M., and Bennett, D. A. (2000). Equilibria, kinetics, and mechanism in the bicarbonate activation of hydrogen peroxide: oxidation of sulfides by peroxymonocarbonate. *J. Am. Chem. Soc.* 122 (8), 1729–1739. doi:10.1021/ja9927467

Ruiz, E. J., Ortega-Borges, R., Jurado, J. L., Chapman, T. W., and Meas, Y. (2009). Simultaneous anodic and cathodic production of sodium percarbonate in aqueous solution. *Electrochem. Solid-State Lett.* 12 (1), E1. doi:10.1149/1.3005555

Russo, V., Tesser, R., Santacesaria, E., and Di Serio, M. (2013). Chemical and technical aspects of propene oxide production via hydrogen peroxide (HPPO process). *Ind. Eng. Chem. Res.* 52 (3), 1168–1178. doi:10.1021/ie3023862

Sato, K. (2004). Green oxidation with aqueous hydrogen peroxide. *AIST Today (International Ed.)* (12), 32. doi:10.5363/tits.14.3_60

Schanz, T., Burek, B. O., and Bloh, J. Z. (2023). Fate and reactivity of peroxides formed over BiVO 4 anodes in bicarbonate electrolytes. *ACS Energy Lett.* 8 (3), 1463–1467. doi:10.1021/acsenergylett.3c00227

Schneider, S., and Stöckl, M. (2024). General route to indirect and on-demand electrosynthesis of (various) peroxy acids via *in situ* generated hydrogen peroxide on a gas diffusion electrode. *ACS Sustain. Chem. Eng.* 12, 5160–5168. doi:10.1021/acssuschemeng.3c07823

Shi, X., Siahrostami, S., Li, G. L., Zhang, Y., Chakthranont, P., Studt, F., et al. (2017). Understanding activity trends in electrochemical water oxidation to form hydrogen peroxide. *Nat. Commun.* 8 (1), 701–712. doi:10.1038/s41467-017-00585-6

Shi, X., Zhang, Y., Siahrostami, S., and Zheng, X. (2018). Light-driven BiVO4–C fuel cell with simultaneous production of H2O2. *Adv. Energy Mater.* 8 (23), 1–9. doi:10.1002/aenm.201801158

Siahrostami, S., Li, G.-L., Viswanathan, V., and Nørskov, J. K. (2017). One- or two-electron water oxidation, hydroxyl radical, or H_2O_2 evolution. *J. Phys. Chem. Lett.* 8 (6), 1157–1160. doi:10.1021/acs.jpclett.6b02924

Siahrostami, S., Villegas, S. J., Bagherzadeh Mostaghimi, A. H., Back, S., Farimani, A. B., Wang, H., et al. (2020). A review on challenges and successes in atomic-scale design of catalysts for electrochemical synthesis of hydrogen peroxide. *ACS Catal.* 10 (14), 7495–7511. doi:10.1021/acscatal.0c01641

Silva, F. L., Reis, R. M., Barros, W. R. P., Rocha, R. S., and Lanza, M. R. V. (2014). Electrogeneration of hydrogen peroxide in gas diffusion electrodes: application of iron (II) phthalocyanine as a modifier of carbon black. *J. Electroanal. Chem.* 722–723, 32–37. doi:10.1016/j.jelechem.2014.03.007

Stöckl, M., Lange, T., Izadi, P., Bolat, S., Teetz, N., Harnisch, F., et al. (2023). Application of gas diffusion electrodes in bioeconomy: an update. *Biotechnol. Bioeng.* 120 (6), 1465–1477. doi:10.1002/bit.28383

Sun, Y., Han, L., and Strasser, P. (2020). A comparative perspective of electrochemical and photochemical approaches for catalytic H2O2 production. *Chem. Soc. Rev.* 49 (18), 6605–6631. doi:10.1039/d0cs00458h

Sun, Y., Sinev, I., Ju, W., Bergmann, A., Dresp, S., Kühl, S., et al. (2018). Efficient electrochemical hydrogen peroxide production from molecular oxygen on nitrogen-doped mesoporous carbon catalysts. *ACS Catal.* 8 (1), 2844–2856. doi:10.1021/acscatal.7b03464

Wenderich, K., Kwak, W., Grimm, A., Kramer, G. J., Mul, G., and Mei, B. (2020). Industrial feasibility of anodic hydrogen peroxide production through photoelectrochemical water splitting: a techno-economic analysis. *Sustain. Energy Fuels* 4 (6), 3143–3156. doi:10.1039/d0se00524j

Wenderich, K., Nieuweweme, B. A. M., Mul, G., and Mei, B. T. (2021). Selective electrochemical oxidation of H2O to H2O2Using boron-doped diamond: an experimental and techno-economic evaluation. *ACS Sustain. Chem. Eng.* 9 (23), 7803–7812. doi:10.1021/acssuschemeng.1c01244

Xia, C., Back, S., Ringe, S., Jiang, K., Chen, F., Sun, X., et al. (2020). Confined local oxygen gas promotes electrochemical water oxidation to hydrogen peroxide. *Nat. Catal.* 3 (2), 125–134. doi:10.1038/s41929-019-0402-8

Xiao, J., Wang, M., Pang, Z., Dai, L., Lu, J., and Zou, J. (2019). Simultaneous spectrophotometric determination of peracetic acid and the coexistent hydrogen peroxide using potassium iodide as the indicator. *Anal. Methods* 11 (14), 1930–1938. doi:10.1039/c8ay02772b

Xue, Y., Wang, Y., Pan, Z., and Sayama, K. (2021). Electrochemical and photoelectrochemical water oxidation for hydrogen peroxide production. *Angew. Chem. - Int. Ed.* 60 (19), 10469–10480. doi:10.1002/anie.202011215

Zhao, S., Xi, H., Zuo, Y., Wang, Q., Wang, Z., and Yan, Z. (2018). Bicarbonate-activated hydrogen peroxide and efficient decontamination of toxic sulfur mustard and nerve gas simulants. *J. Hazard. Mater.* 344, 136–145. doi:10.1016/j.jhazmat.2017.09.055